PHYSICAL REVIEW B **85**, 020102(R) (2012)

Direct observation of interlocked domain walls in hexagonal $R\mathrm{MnO_3}$ (R = Tm, Lu)

Q. H. Zhang,[1] L. J. Wang,[1] X. K. Wei,[1] R. C. Yu,[1,*] L. Gu,[1,2,†] A. Hirata,[2] M. W. Chen,[2] C. Q. Jin,[1] Y. Yao,[1] Y. G. Wang,[1] and X. F. Duan[1]

[1]*Beijing National Laboratory for Condensed Matter Physics, Institute of Physics, Chinese Academy of Sciences, Beijing 100190, China*

[2]*WPI Advanced Institute for Materials Research, Tohoku University, Sendai 980-8577, Japan*

(Received 20 October 2011; published 9 January 2012)

Using state-of-the-art aberration-corrected annular-bright-field and high-angle annular-dark-field scanning transmission electron microscopy, we investigated domain wall structures in multiferroic hexagonal $\mathrm{TmMnO_3}$ and $\mathrm{LuMnO_3}$ ceramics at the atomic scale. Two types of 180° domain walls (DWs), i.e., the transverse and the longitudinal DWs with uniform displacements of $a/3$ and $2a/3$, respectively, were identified along the b direction, which is in agreement with the interlock between the ferroelectric and structural translation domain walls that had been predicted previously. Across the domain wall the arrangement of $\mathrm{MnO_5}$ polyhedra was not found to be inversed, indicating that (i) it has negligible effects on the polarization and (ii) the structures of the neighbor domains with opposite polarizations are not exactly the same. These wall structures are different from the polarization inversion in conventional ferroelectrics and may be used to explain the unusual transport properties and magnetoelectic effects.

DOI: 10.1103/PhysRevB.85.020102 PACS number(s): 77.80.Dj, 68.37.Ma, 75.85.+t

Hexagonal rare-earth (RE) manganites $R\mathrm{MnO_3}$ (R = Ho to Lu, Y, and Sc), such as a typical multiferroic system that is created by the coexistence of magnetism and ferroelectricity, have received much attention because of their wide potential applications such as information storage and because of their intriguing physical properties.[1–10] Despite the fact that the coupling of magnetism and ferroelectricity contains a very attractive physical nature, weak magnetoelectric coupling limits their practical applications; hence it is crucial to enhance the strength of coupling in multiferroics. Microstructurewise, ferroelectric domain structures play a critical role in the magnetoelectric interaction; thus the investigation of domain structures in multiferroics is of great interest from both applied and fundamental physics standpoints. The study of domain structures has become increasingly appreciated for future compact multifunctional devices.[11–15] Attempts in both theory and experiments were carried out to reveal the intriguing nature of domain walls (DWs): It was predicted that the ferroelectric domain wall in magnetoelectrics can be ferromagnetic;[12–14] and unusual transport properties in the domain wall of $\mathrm{YMnO_3}$ and $\mathrm{BiFeO_3}$ (BFO) were also observed.[16,17] However, little is known at present about the interlocked structural and ferroelectric domains, especially on the atomic scale.

$R\mathrm{MnO_3}$, which is isostructural to $\mathrm{YMnO_3}$, is improper ferroelectrics with a Curie temperature T_C that is highly above room temperature and shows antiferromagnetic (AFM) behavior below the Néel temperature. Its ferroelectric polarization is characterized by a buckling of layered $\mathrm{MnO_5}$ polyhedra and displacements of Y ions.[18] One-third downward distortion and two-third upward distortion of RE ions produces ferroelectric polarization along the c axis,[16] as illuminated in Fig. 1(a). Several methods have been used to study the ferroelectric domain structure at the atomic scale, such as negative spherical-aberration imaging (NCSI), exit wave reconstruction, high-resolution transmission electron microscopy (HRTEM), scanning transmission electron microscopy (STEM), etc. Jia *et al.*[19,20] observed directly the electric dipole and continuous electric dipole rotation of $\mathrm{Pb(Zr,Ti)O_3}$ in the vicinity of domain walls by NCSI. Nelson *et al.*[21] used HRTEM to map spontaneous vortex nanodomain arrays at ferroelectric $\mathrm{BiFeO_3}$ heterointerfaces. In addition, STEM offers a unique perspective to image heavy ions due to its Z-contrast characteristic. The recently developed aberration-corrected microscopy allows the determination of the atomic structure and composition at subangstrom resolution: E.g., Chang *et al.*[22] applied Z-contrast imaging to map polarization across the interface of a BFO/$\mathrm{La_{1-x}Sr_xMnO_3}$ (LSMO)/$\mathrm{SrTiO_3}$ (STO) thin film. Here, we apply an aberration-corrected annular-bright-field (ABF) and high-angle annular-dark-field (HAADF) imaging technique to map the atomic shift in the ferroelectric hexagonal $\mathrm{TmMnO_3}$ and $\mathrm{LuMnO_3}$. Ferroelectric DWs in $\mathrm{TmMnO_3}$ and $\mathrm{LuMnO_3}$ ceramics were carefully examined, and two types of DWs corresponding to the uniform displacement of $a/3$ and $2a/3$ across a domain wall were identified, respectively.

Polycrystalline $\mathrm{LuMnO_3}$ and $\mathrm{TmMnO_3}$ samples were synthesized by a conventional solid-state reaction method. A stoichiometric mixture of $\mathrm{Lu_2O_3}$, $\mathrm{Tm_2O_3}$, and $\mathrm{Mn_2O_3}$ powders was well ground and calcined twice in air at 1200 °C for 24 h. Details of the sample preparation can be found elsewhere.[10] The crystal structure refinement was carried out by Wang *et al.*,[10] and the crystal constants were defined as $a = 6.08$ Å and $c = 11.37$ Å. The refinement data were also used to construct the structural model shown in Fig. 1(a). Thin samples for transmission electron microscopy (TEM) were prepared by crushing the grains in an agate mortar filled with alcohol, then dispersing the resulting fine fragments suspended in alcohol on holey carbon films supported by copper grids. ABF and HAADF images were acquired using a JEOL 2100F transmission electron microscope operated at 200 keV at acceptance angles of 12–25 and 70–150 mrad, respectively.

Figure 2(a) shows a lattice image of a typical area including two antiparallel polarization orientations. In Fig. 2, the structure of $\mathrm{TmMnO_3}$ is labeled schematically in two regions. Since the HAADF contrast is generally less affected

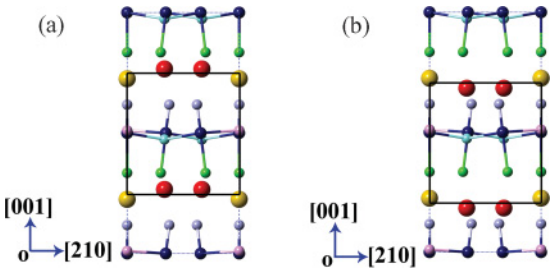

FIG. 1. (Color online) (a) The structure model constructed by x-ray refinement data along the *b* axis. The yellow (light gray) and red (dark) spheres represent Tm1 and Tm2, respectively. The small dark blue (dark) spheres are Mn and the rest are oxygen. The black line rectangle marks the arrangement frame of Tm ions in a paraelectric state. (b) The structure model obtained from (a) changes the RE arrangements corresponding to the opposite polarization.

by a small variation in the specimen thickness, mapping the atomic position of heavier ions using the HAADF approach is a reliable method to measure ion displacements and to calculate further the polarization. The same information was also obtained from an ABF image which is also capable of resolving light atoms [Fig. 2(b)]. Since the situation in $LuMnO_3$ is very similar to that of $TmMnO_3$, we simply present the results of $TmMnO_3$. The different shifts of Tm1 and Tm2 atoms as compared to the MnO_5 polyhedra, which appear wavylike, indicate that $TmMnO_3$ is in a polarized state. The polarization can be visualized by assuming valence charges centered on each of the ion sites. In Van Aken's paper,[18] the off-center shift of Mn ions from the center of O_5 polyhedra is very small, and the polarization along the *c* axis is mainly generated from the relative downward and upward displacements of Tm1 and Tm2 atoms, respectively. We define a vector $\vec{S}_{12}$ as the atomic displacement of Tm1 from the midpoint of two Tm2 neighbors, and $|\vec{S}_{12}|$ in the inner region of the ferroelectric domain is measured to be ~50 pm. The relationship between $\vec{S}_{12}$ and the polarization in the image plane is

$$\vec{P} = \frac{1}{2}\frac{-2 \times 3 \times \vec{S}_{12} \times e}{V} = -0.13\frac{\mu C}{cm^2\ pm} \cdot \vec{S}_{12},$$

where V is the volume of one unit cell of $TmMnO_3$, and e is the charge of one electron. It yields a polarization of 6.5 $\mu C/cm^2$ along the *c* axis, in good agreement with the reported polarization of $YMnO_3$.[18]

In order to highlight the position of the domain wall, we superimpose the structural model of $TmMnO_3$ on the both sides of the image with opposite polarizations. Yellow (light gray) arrows are used to mark the opposite polarization vector in two oppositely polarized regions, and the red (dark) dotted line indicates the position of the domain wall. Similar to the definitions about the types of domain wall in Jia *et al.*,[20] which were categorized as transverse DWs (TDWs) (the polarization direction is perpendicular to the normal of domain wall) and longitudinal DWs (LDWs) (the polarization direction is parallel to the normal of domain wall), we define the two types of domain wall as TDWs and LDWs, although they have important differences in the region of polarization inversion. Figure 3(a) shows an enlarged STEM image of TDWs from Fig. 2(a). On each side, the agreements between the structural model and the *Z*-contrast image is good, which indicates that our experimental image is of high quality and can directly explain the ferroelectric polarization. On the left-hand side of Fig. 3(a), Tm1 displaces upward while Tm2 downward, producing a polarization downward. It is reversed on the right-hand side of Fig. 3(a). The red (dark) dotted line in the middle region indicating the position of the domain wall denotes a transition from negative polarization to positive with a width of $\sqrt{3}a/6$ perpendicular to the TDWs, which corresponds to $a/3$ displacement at the domain wall. Figure 3(b) shows the corresponding ABF image of Fig. 3(a) obtained by converting the grayscale contrast of Fig. 2 to a rainbow-colored (gray) scale to enhance contrast, which was recorded simultaneously with the HAADF image. The contrast between the RE ion rows indicates the arrangement of MnO_5, and obviously no inversion occurs across the domain wall.

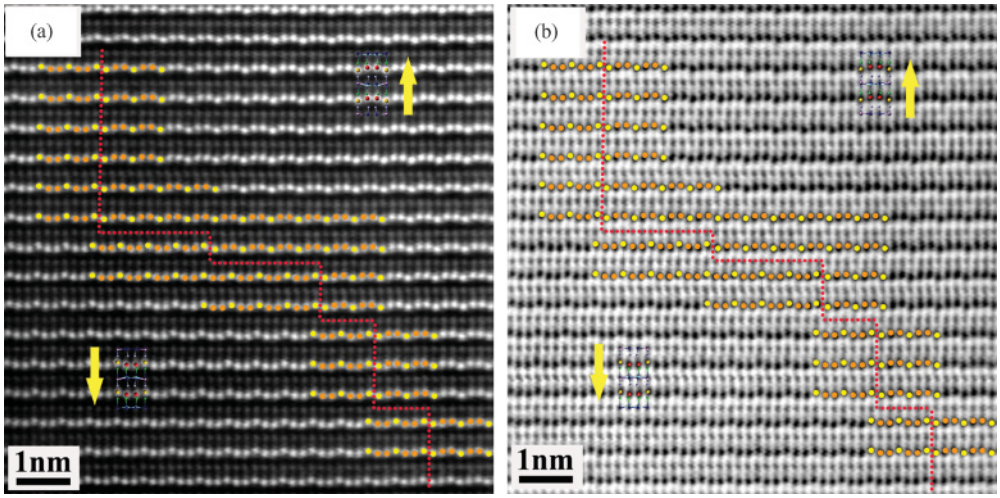

FIG. 2. (Color online) Atomic-resolution HAADF (a) and ABF (b) images of $TmMnO_3$ with a steplike 180° domain wall. The structure model of $TmMnO_3$ is schematically shown in the two regions with opposite polarizations; the positions of Tm1 and Tm2 are indicated by yellow (white) and brown (gray) colors, respectively.

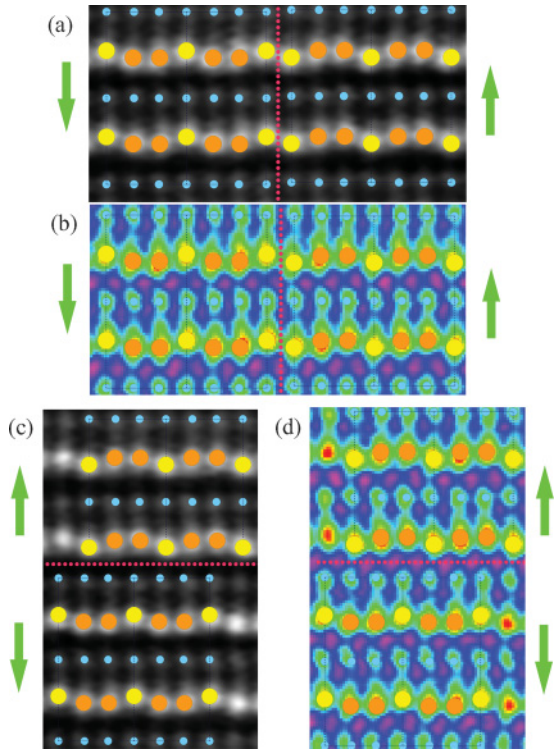

FIG. 3. (Color online) (a) HAADF and (b) ABF images of $TmMnO_3$ exhibiting a TDW with $a/3$ displacement, respectively. (c) HAADF and (d) ABF images of $TmMnO_3$ exhibiting a LDW with $a/3$ displacement, respectively.

Figure 3(c) shows another type of domain wall, i.e., the LDWs. From the image imposed by the structural model, we also found opposite polarizations at both sides of the domain wall, and a displacement of $a/3$ (corresponding to $\sqrt{3}a/6$ in the image) can be recognized between the two opposite polarized regions. The unchanged contrast distribution of MnO_5 across the domain wall is also observed in Fig. 3(d). According to the above ABF observations, we should note an important but interesting phenomenon that the contrast distribution of MnO_5 across the two types of domain walls remains unchanged in our experiments. This is discussed in detail below. The appearance of LDW demonstrates that a domain topology in the plane parallel to the c axis is also allowed.[23] Unlike the TDWs, the displacement direction of the entire structural unit across the domain wall is parallel to the LDWs. Unlike the situation in the $Pb(Zr,Ti)O_3$ described by Jia *et al.*, the polarization inversion here is realized by a displacement perpendicular to the c axis in the TDWs and LDWs. The special effect of the displacement at the domain wall will be mentioned later.

Figure 4 displays another type of translation domain wall with a displacement of $2a/3$. Two schematic models with only heavy atom Tm are superimposed on the two inversely polarized regions marked by two opposite green (gray) arrows. Obviously, this TDW is associated by a displacement of $2a/3$ (corresponding to $\sqrt{3}a/3$ in the image). It is worth mentioning that the TDW with $2a/3$ displacement prefers to emerge at the edge of the specimen in our STEM observations, in contrast to the $a/3$ displacement appearing in the inner region. The different residing position for the $a/3$ and $2a/3$ displacements

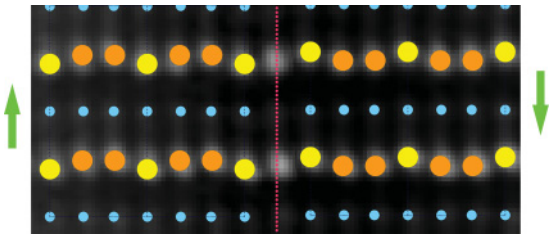

FIG. 4. (Color online) HAADF image of $TmMnO_3$ exhibiting a TDW with $2a/3$ displacement.

is not clear at the moment and its reason needs to be explored by theorists.

As an improper ferroelectrics where the size mismatch between RE and Mn induces a trimerization-type structural phase transition, hexagonal $RMnO_3$ possesses a different nature for the origin of ferroelectricity.[18] Ferroelectricity (FE) in $RMnO_3$ compounds is almost an "accidental by-product" of close packing due to the smallness of the ion radius of Mn.[24] Hence the LDWs and TDWs in hexagonal $RMnO_3$ are naturally translation domain walls,[23] which are called "interlocked" by Choi *et al.*[16] In Choi's paper, they reported six interlocked domain walls and also suggested a structure model, along the view of the c direction, with two types of translation boundaries combined with two opposite polarization domains. In our work, we carried out observations along the direction perpendicular to the c axis, and thus only two types of translation boundaries can be observed, which were indeed captured in our study, demonstrating convincingly their assumption for six domains.

The ABF image technique is capable of resolving light elements. Despite the fact that a single oxygen atom cannot been differentiated in the present orientation, the arrangement of MnO_5 can be characterized. As revealed in Figs. 3(b) and 3(d), the contrast of MnO_5 has no obvious changes in two antiparallel polarized regions, from which two conclusions can be reached. First, MnO_5 has a negligible effect on the formation of ferroelectric polarization, indicating that the arrangement of MnO_5 is not closely correlated to the inversion of polarization, in agreeement with the earlier report[18] about the origin of ferroelectricity in hexagonal $RMnO_3$. Second, as a matter of course, it is ruled out that the structures of the two neighboring domains with opposite polarizations are not exactly the same, as illustrated in Figs. 1(a) and 1(b), respectively.

The reason why a displacement accompanies the polarization inversion can be understood from the perspective of intrinsic structural characters. The FE in hexagonal $RMnO_3$ is accomplished by two parts: One is MnO_5's tilting and buckling that is induced by the large size mismatch, which does not contribute fully to the polarization; and another is the shift of RE ions that is directly induced by tilting and buckling of MnO_5, which contributes mostly to the polarization.[18] Therefore the inversion of polarization is realized mainly by the arrangement variation of RE ions. However, the Coulomb interaction would be too strong should the domains with opposite polarizations have no displacement, which is also energetically unstable. Therefore a mediate state with a displacement is needed for RE ions to release a strong electrostatic repulsive force,[23] and the interlocking between structural translation domain walls

and ferroelectric domain walls (FEWs) is necessary, which is consistent with the earlier paper.[16]

In the family of hexagonal rare-earth manganites $R\mathrm{MnO_3}$, magnetoelectric coupling is symmetry forbidden, however, anomalies in the dielectric constant of $\mathrm{YMnO_3}$ were observed near its Néel temperature,[25] indicating that the magnetoelectric (ME) behavior originates mainly in the clamped wall because of its low local symmetry. The clamping of FEW and AFM order parameters at FEW domain walls in $R\mathrm{MnO_3}$ has been intensively investigated since 2000. It has been confirmed that FEWs are naturally AFMWs below Néel temperature in $\mathrm{YMnO_3}$ by imaging with optical second harmonic generation (SHG),[26] and other hexagonal manganites $R\mathrm{MnO_3}$ were also studied by Hanamura *et al.*[1] Different assumptions were proposed to explain the mechanism of clamping of FEW and AFMW: The Dzyaloshinski-Moriya interaction is considered to be the origin of the clamping;[27,28] the piezomagnetism effect due to the lattice distortion at the ferroelectric domain wall can lower the free energy of the system, favoring coupling between the electric and magnetic domain walls.[29] Now the microstructure of the ferroelectric domain wall is revealed on the atomic scale by aberration-corrected STEM, and it is demonstrated that specific displacements always accompany the DWs to cause the interlocking. The origin of clamping of the FEW and AFMW in such types of domain walls would need to be investigated theoretically.

We have observed two types of interlocked structural translation domain walls and ferroelectric domain walls, which are accompanied by $a/3$ and $2a/3$ displacements, respectively. Across the domain wall the arrangement of $\mathrm{MnO_5}$ is not inversed, indicating that it has a negligible effect on the polarization, and the crystal structures of the neighboring domains with opposite polarizations are not exactly the same. The observed TDW with $2a/3$ displacement prefers to appear at the edge of specimen, whereas the LDW and TDW with $a/3$ displacement prefer to stay at the inner regions. The displacement and polarization inversion are always accompanied, in other words, FEWs are naturally structural translation domain walls, and also AFMWs below Néel temperature.[26] These walls correlate together to determine a great amount of intriguing electrical and magnetic behaviors that are based upon their mutual control.

This work was supported by the National Natural Science Foundation of China (Grants No. 11174336 and No. 50921091), the National Basic Research Program of China (Grant No. 2012CB932302), and the specific funding of Discipline and Graduate Education Project of Beijing Municipal Commission of Education. L.G. is grateful for the support from the "Hundred Talents" program of the Chinese Academy of Sciences.

*rcyu@aphy.iphy.ac.cn

†l.gu@iphy.ac.cn

[1] E. Hanamura and Y. Tanabe, Phase Transitions **79**, 957 (2006).

[2] S. Harikrishnan, S. Rossler, C. M. N. Kumar, H. L. Bhat, U. K. Rossler, S. Wirth, F. Steglich, and S. Elizabeth, J. Phys. Condens. Mater. **21**, 96002 (2009).

[3] T. Katsufuji, M. Masaki, A. Machida, M. Moritomo, K. Kato, E. Nishibori, M. Takata, M. Sakata, K. Ohoyama, K. Kitazawa, and H. Takagi, Phys. Rev. B **66**, 134434 (2002).

[4] T. Katsufuji, S. Mori, M. Masaki, Y. Moritomo, N. Yamamoto, and H. Takagi, Phys. Rev. B **64**, 104419 (2001).

[5] T. Kordel, C. Wehrenfennig, D. Meier, Th. Lottermoser, M. Fiebig, I. Gelard, C. Dubourdieu, J. W. Kim, L. Schultz, and K. Dorr, Phys. Rev. B **80**, 045409 (2009).

[6] T. Lonkai, D. G. Tomuta, U. Amann, J. Ihringer, R. W. A. Hendrikx, D. M. Tobbens, and J. A. Mydosh, Phys. Rev. B **69**, 134108 (2004).

[7] T. Lottermoser and M. Fiebig, Phys. Rev. B **70**, 220407 (2004).

[8] C. Y. Ren, Phys. Rev. B **79**, 125113 (2009).

[9] Y. Tokura, J. Magn. Magn. Mater. **310**, 1145 (2007).

[10] L. J. Wang, S. M. Feng, J. L. Zhu, R. C. Yu, and C. Q. Jin, Appl. Phys. Lett. **91**, 172502 (2007).

[11] L. Thomas, M. Hayashi, X. Jiang, R. Moriya, C. Rettner, and S. Parkin, Science **315**, 1553 (2007).

[12] J. Privratska and V. Janovec, Ferroelectrics **204**, 321 (1997).

[13] J. Privratska and V. Janovec, Ferroelectrics **222**, 281 (1999).

[14] A. V. Goltsev, R. V. Pisarev, T. Lottermoser, and M. Fiebig, Phys. Rev. Lett. **90**, 177204 (2003).

[15] M. Mostovoy, Phys. Rev. Lett. **96**, 067601 (2006).

[16] T. Choi, Y. Horibe, H. T. Yi, Y. J. Choi, W. D. Wu, and S. W. Cheong, Nat. Mater. **9**, 253 (2010).

[17] J. Seidel, L. W. Martin, Q. He, Q. Zhan, Y.-H. Chu, A. Rother, M. E. Hawkridge, P. Maksymovych, P. Yu, M. Gajek, N. Balke, S. V. Kalinin, S. Gemming, F. Wang, G. Catalan, J. F. Scott, N. A. Spaldin, J. Orenstein, and R. Ramesh, Nat. Mater. **8**, 229 (2009).

[18] B. B. Van Aken, T. T. M. Palstra, A. Filippetti, and N. A. Spaldin, Nat. Mater. **3**, 164 (2004).

[19] C.-L. Jia, S.-B. Mi, K. Urban, I. Vrejoiu, M. Alexe, and D. Hesse, Nat. Mater. **7**, 57 (2008).

[20] C. L. Jia, K. W. Urban, M. Alexe, D. Hesse, and I. Vrejoiu, Science **331**, 1420 (2011).

[21] C. T. Nelson, B. Winchester, Y. Zhang, S. J. Kim, A. Melville, C. Adamo, C. M. Folkman, S. H. Baek, C. B. Eom, D. G. Schlom, L. Q. Chen, and X. Q. Pan, Nano. Lett. **11**, 828 (2011).

[22] H. J. Chang, S. V. Kalinin, A. N. Morozovska, M. Huijben, Y. H. Chu, P. Yu, R. Ramesh, E. A. Eliseev, G. S. Svechnikov, S. J. Pennycook, and A. Y. Borisevich, Adv. Mater. **23**, 2474 (2011).

[23] T. Jungk, A. k. Hoffmann, M. Fiebig, and E. Soergel, Appl. Phys. Lett. **97**, 012904 (2010).

[24] D. I. Khomskii, J. Magn. Magn. Mater. **306**, 1 (2006).

[25] Z. J. Huang, Y. Cao, Y. Y. Sun, Y. Y. Xue, and C. W. Chu, Phys. Rev. B **56**, 2623 (1997).

[26] M. Fiebig, T. Lottermoser, D. Frohlich, A. V. Goltsev, and R. V. Pisarev, Nature (London) **419**, 818 (2002).

[27] E. Hanamura, K. Hagita, and Y. Tanabe, J. Phys. Condens. Matter **15**, 103 (2003).

[28] E. Hanamura and Y. Tanabe, J. Phys. Soc. Jpn. **72**, 2959 (2003).

[29] Z. Wang, F. Z. Huang, X. M. Lu, and J. S. Zhu, Eur. Phys. J. B **75**, 217 (2010).